

Insights into Structure and Mechanical Behavior of α and γ Crystal Forms of Nylon-6 at Low Strain by Infrared Studies

Leslie S. Loo and Karen K. Gleason*

Department of Chemical Engineering, Massachusetts Institute of Technology, Cambridge, Massachusetts 02139

Received February 18, 2003; Revised Manuscript Received May 7, 2003

ABSTRACT: Stress-induced frequency shifts of spun-cast nylon-6 films with α and γ crystals are studied at low strains with particular emphasis on vibrations related to hydrogen bonding and to the methylene chains. With increasing stress in the α films, there is a frequency increase of the NH stretching mode in the crystals where the NH bonds are preferentially aligned parallel to the tensile stretching direction. The CH₂ stretching modes undergo a downward shift. This is correlated with the weakening of the hydrogen bonds and opening up of the tightly packed α crystal structure during deformation, thereby increasing both the N–H–O and CH bond lengths. In the α crystals where the NH bond and stretching directions are perpendicular to each other, compressive forces do not lead to significant amounts of frequency shifting of the NH stretching peak. Tensile deformation has less effect in weakening the hydrogen bonds in the more dynamic amorphous regions. For the γ films, however, there is negligible frequency shift of the NH and CH₂ stretching modes with deformation. The high sensitivity of the NH stretching frequency to mechanical stress (frequency shift coefficient, $\alpha = 100 \text{ cm}^{-1}/\text{GPa}$) demonstrates the utility of using FTIR to study deformation micromechanics in hydrogen-bonded systems. An analysis was performed utilizing bond potentials which revealed that the observed FTIR shifts correspond to changes in X–H bond distances that are as small as 0.001%.

1. Introduction

Nylon-6 is an important engineering plastic which has been extensively studied in terms of its structure and mechanical properties. The elastic moduli of the α crystals have been experimentally evaluated by various authors.^{1–4} Ward has also performed a similar analysis on the γ crystals.⁵ The moduli of the amorphous regions have been studied by Prevorsek et al.⁶ There have also been computational evaluations of the moduli of the crystalline regions.^{7–9}

Extensive literature also exists for large strain studies of nylon-6. Plastic deformation mechanisms have been studied by Galeski et al.,^{10–12} and Lin and Argon have established the principal slip planes under plastic deformation.¹ Murthy et al. have examined the deformation of the lamella structure¹³ and structure–property relationship of nylon-6 fibers.¹⁴ Recently, Penel-Pierron et al. have investigated the large strain deformation of nylon-6 films using FTIR.¹⁵ Most of these studies focused on how deformation caused changes in the morphology such as breakup of crystals, transformation of one crystalline form to another, and orientation effects. The methods commonly used are wide-angle X-ray scattering (WAXS), small-angle X-ray scattering (SAXS), and transmission electron microscopy (TEM).

In this work, FTIR is used to study molecular events such as changes in local configurations, bond lengths, bond angles, and atomic interactions during deformation in the low strain regime (up to 10% strain). This cannot be achieved with bulk techniques such as WAXS, SAXS, and TEM. Even though it has been possible to obtain changes in d spacing of different planes in polymeric crystals by X-ray techniques,² it is more difficult to probe molecular changes in the crystalline as well as amorphous regions at low strains. X-ray scattering cannot pick up hydrogen atoms and hence cannot give information about X–H bond lengths. Thus, a spectroscopic

method such as FTIR, which is sensitive to local bonding environments and conformation, is needed. Changes are revealed by stress-induced frequency shifts in FTIR. Such peak shifts in FTIR have first been studied by Zhurkov and co-workers to find out how the applied mechanical stress imposed upon a sample is distributed among the interatomic bonds.^{16–18} Later investigators utilized FTIR peak shifts to gain an understanding of the molecular mechanism of deformation in highly drawn polymers such as polypropylene, polyethylene, and polyoxymethylene.^{19–21} The peak shift is directly proportional to the applied stress as follows:

$$\Delta\nu = \alpha\sigma \quad (1)$$

where $\Delta\nu$ is the peak shift, α is a proportionality constant, and σ is the stress. To date, no such analysis has been done for nylon-6, although dynamic FTIR studies have been carried out.^{22,23} Zhurkov et al.'s earlier work on highly drawn nylon-6 has focused only on the 930 cm^{-1} crystalline band. Another early work on nylon material was a compression study of nylon-6,6.²⁴ Our work differs in that we did not use highly drawn films, and we investigated stress-induced frequency shifts, due to tensile deformation, of vibrational peaks related to hydrogen bonding which has not been studied before in any polymer.

Nylon-6 forms two types of crystals: α ²⁵ and γ .²⁶ In the α form, the chains lie in an extended zigzag planar fashion. Hydrogen bonds are formed between adjacent antiparallel chains to make up a sheet. The crystal then consists of such hydrogen-bonded sheets stacked upon one another. On the other hand, in the γ form, the hydrogen bonds are formed between the sheets, between parallel chains. The calculated H:H distance between methylene groups on adjacent chains is much shorter in the α crystals (2.140 Å) than in the γ crystals (2.466 Å) to permit optimal hydrogen bonding between the

amide and carbonyl unit.⁸ In polyethylene, where the packing of methylene units is optimal, the minimum distance of 2.447 Å is close to that of the γ crystals, hence reflecting less repulsion between methylene units on adjacent γ chains compared to the α crystals.

2. Experimental Section

Nylon-6 pellets were obtained from UBE Industries. The grade was 1022B (homopolymer, molecular weight $\sim 22\,000$, basic grade). The pellets were dried in a vacuum oven for more than 24 h at room temperature and then stored in a desiccator. To produce thin films suitable for FTIR measurements, the pellets were first dissolved in 2,2,2-trifluoroethanol (0.5–0.7 g of nylon-6 in 10 mL of solvent), and the solution was spun-cast onto a Teflon substrate with a flat surface. The solvent was removed by heating the film and substrate in a vacuum between 75 and 80 °C for more than 12 h. The resulting film contains primarily α crystals and could be easily peeled off the substrate. Films of two different thicknesses were made for the samples with α crystals. The thicker ones were deuterated while the thinner ones were not deuterated. Samples with predominantly γ crystals were made by subjecting the spun-cast films to the standard iodine treatment.²⁷ Deuterated films were prepared by immersing them in D₂O for at least 2 weeks at room temperature. Excess water was removed by drying the films under vacuum at room temperature for at least 48 h. Murthy et al. have shown that D₂O penetrates into the amorphous regions and exchanges with the NH groups therein and that D₂O does not penetrate into the crystalline phases;²⁸ hence, only the amide sites in the amorphous regions are deuterated.

FTIR Experiment. A Nicolet Nexus 870 FTIR spectrometer equipped with a commercial stretching device (manufactured by Manning Applied Technology) was used to perform the stretching experiments. The detector is MCTA with a range of 650–4000 cm⁻¹. The resolution was 4 cm⁻¹. Films of nominal gauge length 10 mm and width of 10 mm were used. The thickness of films, measured with a digital micrometer at the end of the experiment (to prevent creasing on the deformation), was between 5 and 7 μ m. The film was held between two jaws, and 10 spectra of 64 scans each was taken of the unstretched film. The average position of each peak and the corresponding standard deviation were then determined. The latter number was then taken to be the error of each peak position. Next, with one of the jaws fixed in position, the film was manually stretched in increments of 0.05 mm by means of a micrometer attached to the other jaw. After stretching the film to a new position, it was allowed to relax for 5 min (to allow for purging in order to obtain better signal-to-noise ratio) before the spectrum of 64 scans was collected. Each spectrum was zero-filled twice, and the peak picking routine in the Omnic version 6 software was used to locate the position of each peak. No baseline correction is applied since only the frequency shifts were of interest and only minute changes in the spectra were observed even up to the highest strain (defined as the change in length of the sample divided by the original length) of about 0.1. At least two sets of experiments were performed on each type of film to ensure reproducibility. All experiments were carried out at room temperature. To monitor the degree of exchange of the deuterated sites with water vapor in the sample compartment, control experiments were also performed whereby the deuterated samples were simply held in the jaws without being stretched and infrared spectra were taken (at similar time intervals as the stretching experiments).

Polarized spectra were obtained in a similar manner with the polarizer direction parallel and perpendicular to the stretching direction.

For trichroic (three-dimensional orientation) measurements, infrared spectra in the thickness direction were obtained by the sample-tilting procedure described by Schmidt.²⁹ A custom-made device was used to rotate the films around a vertical axis. Refractive index measurements were obtained from vertically polarized spectra of the films aligned normal to and

at angles of -45° and 45° to the infrared beam direction. The spectra in the thickness direction were then calculated from horizontally polarized spectra of the films aligned normal to and at angles of -45° and 45° to the beam.

WAXS $2\theta/\theta$ measurements were performed on a Rigaku RU300 X-ray generator with Cu K α radiation at a voltage of 60 kV and a current of 300 mA. The Bragg angle θ was determined to be the angle which the X-ray beam made with the surface of the films.

Tensile measurements were carried out on an Instron instrument. The elongation rate was 1.0 mm/min. The modulus of the films with primarily α crystals was 427–600 MPa. Films with γ crystals had a modulus of 106–184 MPa.

Density measurements were carried out using a density gradient column filled with toluene and carbon tetrachloride at 22.5 °C. The positions of the films in the column were recorded 24 h after immersion. The density of the α crystals, γ crystals, and amorphous regions are taken to be 1.24, 1.17, and 1.09 g/cm³, respectively.³⁰ The percentage crystallinity by volume of the films, χ , was then calculated from

$$\chi = (\rho - \rho_a)/(\rho_c - \rho_a) \quad (2)$$

where ρ is the density of the film, ρ_a is the density of the amorphous regions, and ρ_c is the density of the crystalline regions. The crystallinity of the films containing primarily α crystals was determined to be 46% (thick films) and 38% (thin films). The γ films have a crystallinity of 67%.

3. Results and Discussion of Nylon-6 Film Structure

3.1. Film Structure from X-ray and Trichroic Measurements. Figure 1a shows the X-ray intensity vs 2θ plots of the films containing primarily α phases. There is a strong reflection at about $2\theta = 23.9^\circ$ with a broad shoulder extending to 19° . The peak at 23.9° corresponds to the (002) hydrogen-bonded planes in the α crystals. A sample with isotropic arrangement of α crystals should show reflections of about equal intensity from both the (002) and (200) planes which give a peak at 20° .¹ Since the reflection from the (200) planes were suppressed in the spun-cast film, this indicates that there is a preferential arrangement of hydrogen-bonded planes parallel to the surface of the film. The infrared spectra of the films in the thickness direction were calculated to confirm this observation. The refractive index, n , based on the NH stretching mode in the 3300 cm⁻¹ region was calculated from

$$n = \frac{\sin(\alpha_t)}{\sqrt{1 - \left(\frac{A_y}{A_{yp}}\right)^2}} \quad (3)$$

where A_y is the vertically polarized spectrum with the film normal to the beam, A_{yp} is the vertically polarized spectrum with the film tilted at α_t to the beam, α_t is the angle of tilt. The refractive index of air is taken to be 1.0. The spectrum in the thickness direction A_z can then be calculated from the following formula:

$$A_z = \frac{A_t \sqrt{1 - \frac{\sin^2(\alpha_t)}{n^2}} - A_x}{\left[\frac{\sin^2(\alpha_t)}{n^2} \right]} + A_x \quad (4)$$

where A_x is the horizontally polarized spectrum of the film normal to the beam and A_t is the horizontally

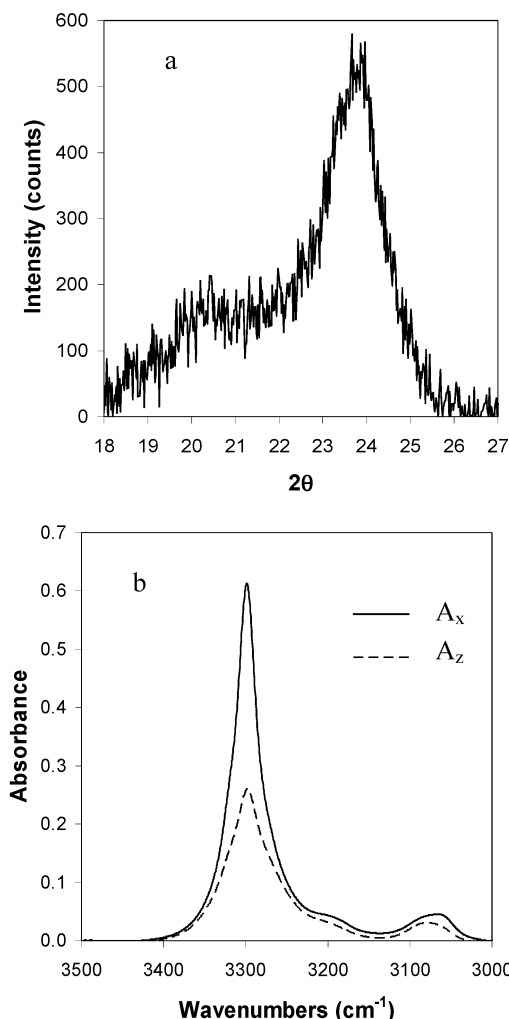


Figure 1. (a) WAXS and (b) infrared spectra of nylon-6 films containing predominantly α crystals (thin α films). The infrared spectra show the NH stretching mode with the solid and dotted lines representing the A_x and A_z spectra, respectively.

polarized spectrum of the film tilted at α_t to the beam. The refractive index is calculated to be 1.66, which is similar to the value of 1.62 in the literature.³¹ The results are shown in Figure 1b. The A_x and A_y spectra are virtually identical, showing that there is no preferential alignment of the NH bonds in the plane of the film. However, the intensity of the NH stretching vibration in the A_z spectrum is half of that in the A_x spectrum. Since the structural absorbance, A_0 , is given by

$$A_0 = (A_x + A_y + A_z)/3 \quad (5)$$

this shows that the NH bonds are preferentially aligned parallel to the plane of the film. It is not possible to perform a similar analysis for the C=O stretching mode because it is over-absorbing ($A > 1$). Since the NH groups are involved in hydrogen bonding, we may therefore conclude that the hydrogen bonds are also preferentially aligned parallel to the film surface but randomly oriented in this plane, supporting the WAXS results. We have found out that solvent casting of the films also produced similar results; thus, such a preferred orientation was not a consequence of the spin-casting process and could be attributed to a thermodynamically favored process.

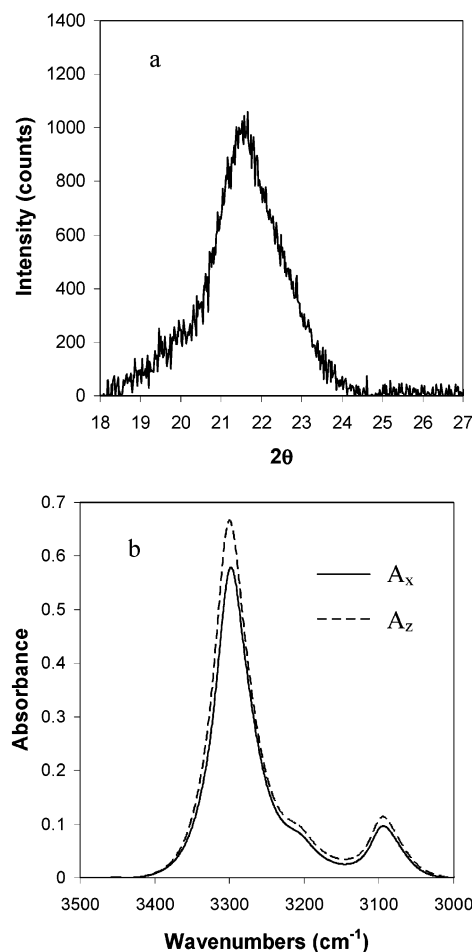


Figure 2. (a) WAXS and (b) infrared spectra of nylon-6 films containing predominantly γ crystals. The infrared spectra show the NH stretching mode with the solid and dotted lines representing the A_x and A_z spectra, respectively.

The films with γ crystals (Figure 2a) showed a strong reflection at $2\theta = 21.5^\circ$ due to the (200) hydrogen-bonded planes. The A_x and A_z infrared spectra of the NH stretching mode are shown in Figure 2b. The refractive index was calculated to be 1.58. The A_x and A_y spectra are identical, and the NH stretching maximum is slightly higher in the A_z spectrum than the A_x spectrum. Hence, the NH bonds are virtually randomly oriented in these films, leading to random orientation of the hydrogen bonds in the γ crystals.

These samples are substantially different from the ultradrawn polymers in the investigations by Wool et al.^{19,20} and Tashiro et al.²¹ because it was difficult to obtain highly drawn films of nylon-6 thin enough to give an NH stretching peak intensity of 1 absorbance unit or below.

3.2. Nylon-6 Conformation. Figure 3a shows the FTIR spectra in the NH stretching region of nylon-6 containing primarily α crystals. This peak is quite broad, indicating that there is a distribution of NH stretching vibrations corresponding to different hydrogen bond strengths in both the crystalline and amorphous regions.³² The absence of any free NH stretching peaks in the 3400 cm^{-1} region shows that all the NH groups are involved in hydrogen bonding. Upon deuteration, the area under the NH stretching peak in this region now corresponds to contributions from primarily the α crystals.²⁸ The fwhm (full width at half-maximum) of the NH stretching peak decreases, and the peak

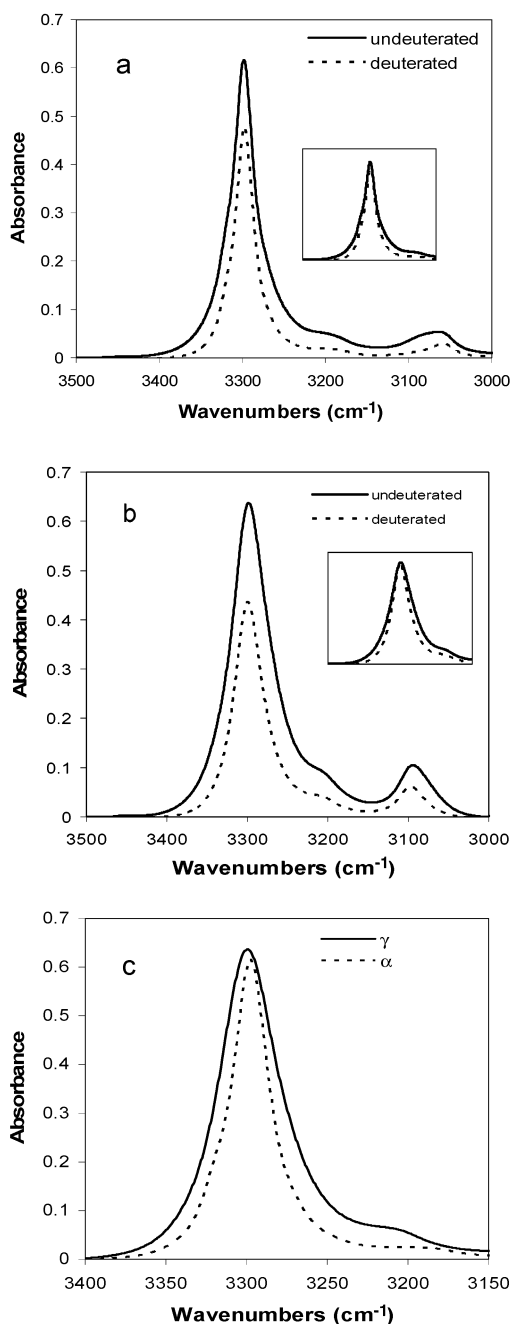


Figure 3. FTIR spectra in the NH stretching region of nylon-6 films containing primarily (a) α crystals and (b) γ crystals. The dotted curves show the FTIR spectra of the deuterated films. The insets show the two curves normalized by peak height. (c) shows the FTIR spectra of the deuterated nylon-6 films.

position shifts from 3299 cm^{-1} to a slightly lower frequency at 3298 cm^{-1} . The NH groups in the amorphous regions, which have undergone exchange to become ND groups, have their ND stretching vibrations showing up as a doublet at 2413 and 2469 cm^{-1} .

A similar phenomenon is also seen for the FTIR spectra of nylon-6 with predominantly γ crystals as shown in Figure 3b. There is a distribution of NH stretching vibrations in the crystalline and amorphous regions. No "free" NH is observed. After deuteration, the NH stretching peak corresponds to NH stretching in primarily the γ crystals. The fwhm of the NH peak decreases, but the peak position shifts about 1 cm^{-1} toward higher wavenumbers, a trend opposite to that of the α films. From Figure 3c, it is observed that the

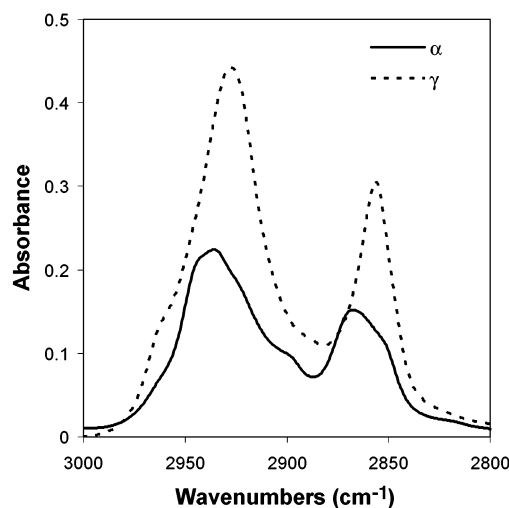


Figure 4. FTIR spectra in the CH_2 stretching region of nylon-6 films containing primarily α (solid line) and γ (dotted line) crystals.

NH stretching peak of the γ crystals is broader than that of the α crystals, indicating that there is a narrower distribution of hydrogen bond strengths in the α than in the γ crystals. The fact that both the α and γ crystals have their NH stretching peak at almost the same location is interesting since the α form is thermodynamically more stable than the γ form, and computer simulation shows that the strongest hydrogen bonds are formed by the α crystals.⁸ There are two possible reasons for this: (a) the peak maximum simply represents contribution from a fairly broad distribution of hydrogen bond lengths and angles; (b) the NH stretching frequency depends on the N–H bond length, N–H...O bond length, H...O bond length, N–H...O bond angle, and the distribution of charges on the N, H, and O atoms which would be a result of the configuration of the chain. All these factors could result in both peaks having the same frequency. Hence, the position of the NH stretching peak per se is not necessary a true reflection of the hydrogen bond strength.

Figure 4 shows the FTIR spectra of the CH_2 asymmetric (higher frequency) and symmetric stretching vibrations. Both peaks in the film with γ crystals are located at lower frequencies than the corresponding peaks of the film containing α crystals. On closer observation, two interesting features can be clearly discerned for the film with α crystals: (a) the CH_2 asymmetric stretching peak is broader than that of the film with γ crystals; (b) this peak also appears to be a composite peak containing several Lorentzian (or Gaussian) peaks superposed together, whereas the peak of the γ film appears to be composed of only one Lorentzian (or Gaussian) peak with a shoulder on the high-frequency side. The same phenomenon is also seen in the CH_2 symmetric stretching vibration for the α and γ films. This can be rationalized as follows: the CH_2 stretching peaks in the γ film contain contributions from the both amorphous and crystalline material. The packing of the methylene chains in γ crystals is optimal,⁸ similar to that in the amorphous regions. Hence, the peaks from the γ crystals and amorphous region coincide. However, the tighter packing of the methylene chains⁸ in the α crystals would result in shorter C–H bonds, a higher force constant for the C–H bond, and hence higher vibrational frequencies for both the CH_2 asymmetric and symmetric stretching modes. Thus,

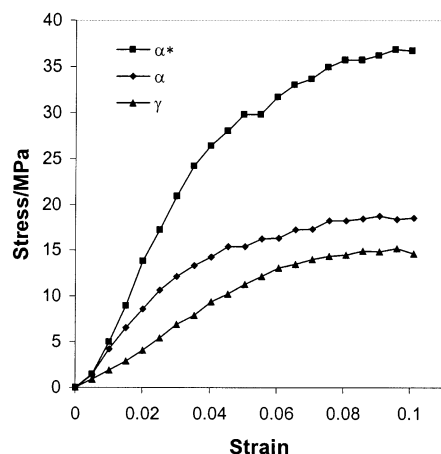


Figure 5. Stress-strain curve of nylon-6 films containing primarily α (diamond), γ (triangle) crystals, and deuterated films containing α crystals (square).

there are at least two components to each CH_2 peak in the α films: the lower frequency one due to the amorphous region and the higher frequency one due to the crystalline phase.

4. Results from Deformation Experiments

Figure 5 shows the engineering stress vs engineering strain curve of the nylon-6 samples used in the experiments. The stress here refers to the stress of the sample at each strain after 5 min of purging has occurred. The curves are linear up to a strain of 0.04, after which more curvature is observed.

4.1. NH and ND Stretching Modes. Figure 6a shows the shape of the NH stretching peak of the deuterated nylon-6 films containing primarily α crystals at strains of 0, 0.02, 0.04, and 0.1. The entire peak shifts to higher frequencies with increasing stress (or strain). Since the NH groups in the amorphous regions are deuterated,²⁸ the area under the NH band represents contributions from the crystals. The change in band shapes indicates that the crystals are involved in deformation. As virtually all the NH groups participate in hydrogen bonding, the shift toward higher frequencies indicates that the hydrogen bonds are weakened during deformation. The decrease in peak height with strain could be attributed to sample thinning.

Figure 6b shows the NH stretching peaks at the same strains but with the height normalized and shifted so that the center frequencies coincide. The fwhm increases with increasing strain, implying that the distribution of hydrogen bond strengths increases with strain. The same phenomena have been observed for nylon-11 heated to higher temperatures.³² The upward shift of the NH stretching mode has been attributed to the weakening of the hydrogen bonds at higher temperatures. Hence, it can also be concluded that during tensile deformation there is weakening of the hydrogen bonds, causing the NH stretch peak to shift toward higher frequencies. The frequency shift can be directly correlated to the tensile deformation process since there is preferential alignment of the hydrogen-bonded planes parallel to the film surface as seen in the WAXS and trichroic data. Therefore, both increasing temperature and mechanical deformation have the same effect of weakening hydrogen bonds and broadening the bond strength distribution.

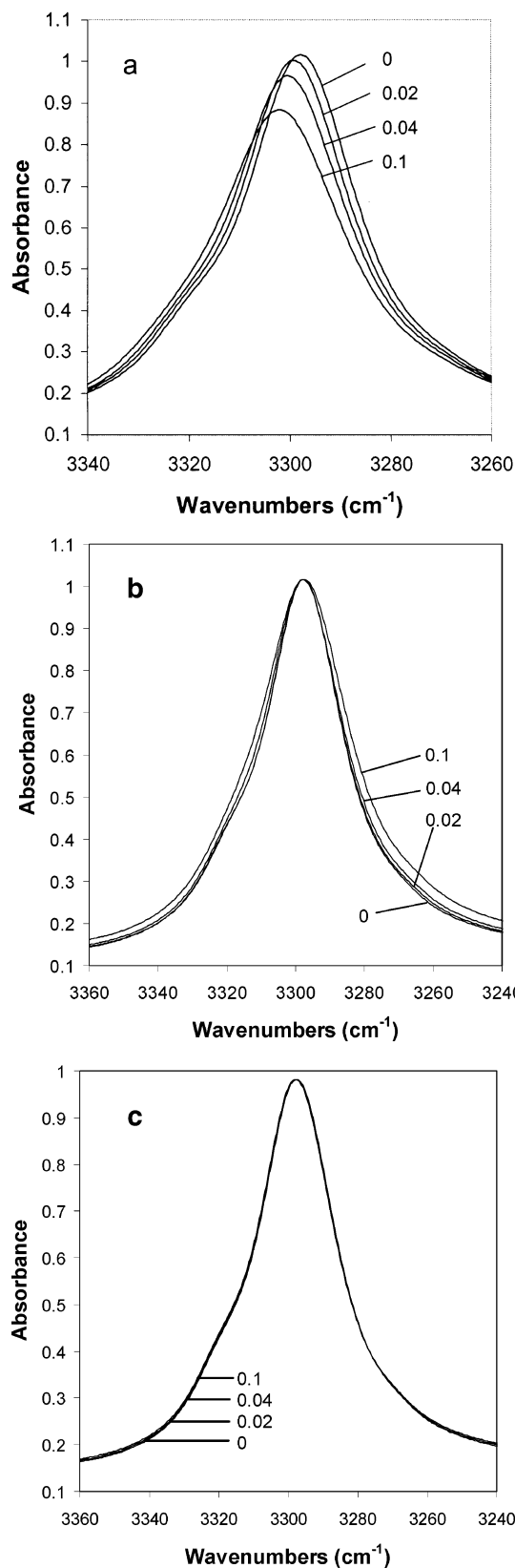


Figure 6. FTIR spectra of the NH stretching region of deuterated nylon-6 films containing primarily α crystals at different strains: (a) without normalization; (b) normalized by peak height and shifted so that the peak frequencies at different strains coincide. The control is shown in (c). For the control curve, as the sample was not stretched; each spectrum is plotted at the strain corresponding to the same point in time of the experimental progress.

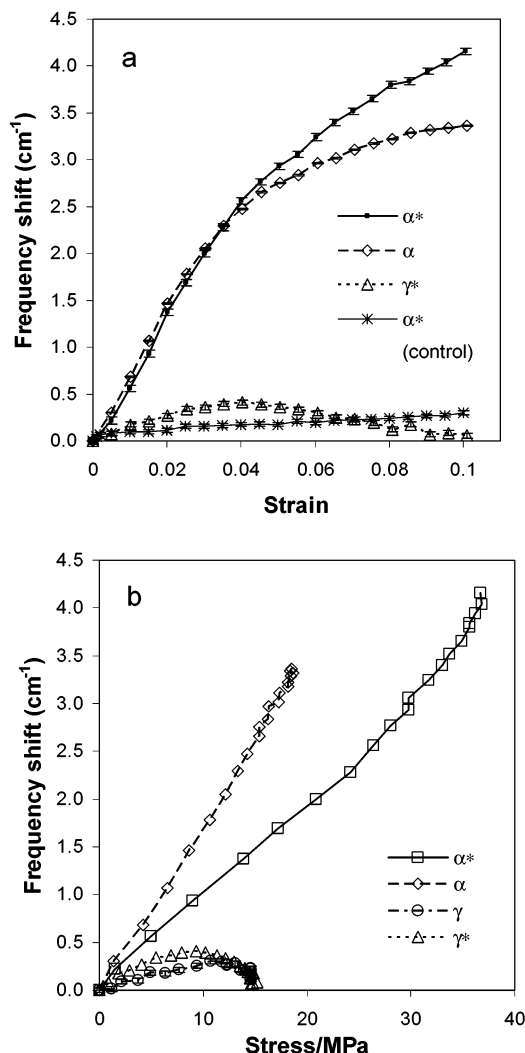


Figure 7. Plot of frequency shift of NH stretching vibration in nylon-6 films vs (a) strain and (b) stress. The asterisks indicate deuterated films. For the control curve, as the sample was not stretched, each point is plotted at the strain corresponding to the same point in time of the experimental progress. The error bars are also shown for each curve.

Figure 6b also shows that the high-frequency shoulder becomes less discernible at higher strains, possibly due to broadening of peak. A slight asymmetry of the peaks is observed at higher strains, with the larger shape change on the lower frequency side. Such an asymmetry has been observed for CC stretching bonds in highly oriented isotactic polypropylene films and has been attributed to a nonuniform distribution of stress among the CC bonds.³³ Figure 6c shows the results of the control experiment for the deuterated α film. The peak heights are normalized (no frequency shifting was performed). There is slight exchange of the ND groups in the amorphous regions with water vapor in the sample compartment, resulting in a small increase of the NH stretching peak height and a slight broadening of this peak. However, this was not sufficient to account for the magnitude of the broadening in Figure 6b.

Figure 7a shows the graph of NH stretching frequency shift vs strain for nylon-6 films. The peak shift is positive and linear for the films with α crystals up to a strain of 0.04 and increases more slowly with strain beyond this strain value. This implies that the force constant of the NH stretching vibration is increasing

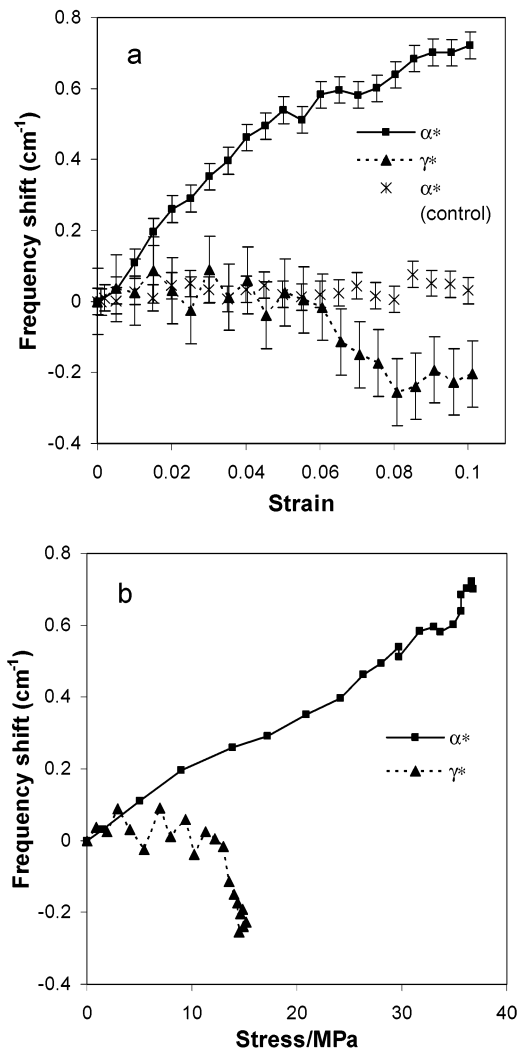


Figure 8. Plot of frequency shift of ND stretching vibration in the amorphous regions of nylon-6 films vs (a) strain and (b) stress. The asterisks indicate deuterated films. For the control curve, as the sample was not stretched, each point is plotted at the strain corresponding to the same point in time of the experimental progress. The error bars are also shown for each curve.

as a result of the weakening of the hydrogen bond. The results of the control experiment indicated that the small degree of exchange between the N-D groups in the amorphous regions and water vapor in the sample compartment caused a slight increase of the NH stretch absorbance and positive frequency shift with time. However, compared to the magnitude of the NH stretch frequency shift, this error is small (less than 8%).

As the hydrogen bond vectors make different angles with respect to the direction of deformation, the NH peak simply reflects the peak maximum of such a distribution. In the nondeuterated films the NH stretching peak reflects contributions from both the crystalline and amorphous regions. Figure 7b shows the NH stretch frequency shift vs stress curves. A linear relationship is observed at all stress values, indicating that the hydrogen bonds are directly bearing the load.

Figure 8a shows the frequency shift for the ND stretching mode at 2469 cm⁻¹ in the amorphous regions. In the α films, the peak shifts toward higher frequencies with strain. The curve is linear up to a strain of 0.04, and the slope decreases at higher strains. This indicates that there is also some weakening of the hydrogen bonds

in the amorphous regions in the α films as a result of the deformation. The amount of shift in the amorphous regions is much less than that in the crystalline regions (Figure 7a), even when taking into account the isotope effect. (A frequency shift of 4 cm^{-1} for the NH stretch should correspond to a frequency shift of 3 cm^{-1} for the ND stretch.) Furthermore, unlike the NH peak of the crystalline regions which broadens with strain, the ND shows negligible changes in peak line width. The peak shift of the α film varies linearly with stress as shown in Figure 8b.

Kischel et al. have obtained polarized spectra of nylon-6 films at a strain of about 0.4% from dynamic FTIR experiments.²² They observed a bipolar peak in the NH stretch region when the polarizer is placed parallel to the stretching direction and a much smaller monopolar peak with the polarizer rotated 90° . They concluded that only the hydrogen bonds that are aligned almost parallel to the external perturbation are affected by the periodic stress. Later, Chase and Ikeda performed dynamic dichroism studies on nylon-6 and showed similar results.²³ They postulated that the hydrogen bonds are dynamic, constantly being made and broken, and that stress transfer could occur between two chains through a hydrogen bond. Such a process would also tend to align the hydrogen bond along the direction of the stress. Kischel et al. as well as Chase and Ikeda did not characterize nor deuterate their nylon-6 samples.

By deuterating the nylon-6 samples, it was possible to distinguish how the α crystals and amorphous regions affect the frequency shift and line width of the NH peak during deformation. The frequency shifts data in Figures 7 and 8 are consistent with the bipolar peaks obtained by the other authors. Furthermore, our results show that it is the NH groups in the α crystals which contribute primarily to the NH peak shift which was reported in the earlier papers. In the elastic regime, a crystal can undergo either rotation, shear, or interplanar separation or a combination of these. Pure rotation alone would not affect the hydrogen bond distances regardless of how the crystal is oriented. Thus, there would be no change in the frequency of the NH stretching mode. Shearing (or some combination of shear and the other two processes) would increase the hydrogen bond distance if the crystal is oriented in the right direction relative to stretching direction, hence increasing the NH stretch frequency. The same effects hold for interplanar separation which results in an increase in the distance between two chains hydrogen-bonded to each other. The authors believe that this is what is happening in these films. Since the deformation occurred at a much lower temperature than the melting point of the α crystals (260°C),³⁰ it is unlikely that the mechanism of stress transfer postulated by Chase and Ikeda could occur in the crystals.

The question then arises whether the hydrogen bonds of all the crystals in the film are affected similarly by the tensile deformation. To answer this question, the results from the polarized FTIR spectra were utilized. Figure 9 shows the frequency shift data of the NH stretching peak of the undeuterated thin α films. Although this peak contains contributions from both the amorphous and crystalline regions, the effects of the amorphous regions are minimal since the authors have shown earlier that the frequency shifts of the NH vibrations in the amorphous regions are much smaller

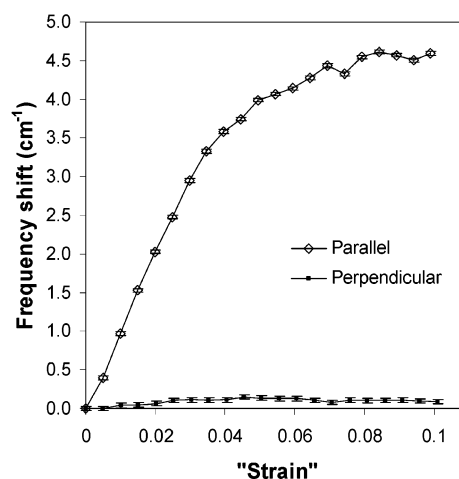


Figure 9. Plot of the frequency shift of the NH stretching vibration in thin undeuterated nylon-6 α films vs strain. The open diamond and closed circle symbols are for the spectra taken with the polarizer parallel and perpendicular to the stretching direction, respectively. The error bars are also shown for each curve.

compared to those in the crystalline regions. Figure 9 indicates that the frequency shifts are seen primarily in the spectra where the polarizer direction is parallel to the stretching direction. The main contribution to the NH frequency shift comes from the crystals in which the NH bonds are aligned parallel or nearly parallel to the stretching direction. This result is similar to the conclusions drawn by Kischel et al.²²

Under uniaxial tensile loading the film will extend in the direction of the stress but contract in the other two orthogonal directions. Since the Poisson ratio of nylon-6 is 0.33,³⁰ there will be an overall increase in volume of the specimen at small extensions. Our results indicate that the Poisson effect alone is not sufficient to account for the weakening of the hydrogen bond and shifting the NH stretching band to higher frequencies. Instead, there must be favorable alignment of the hydrogen bond in the crystal relative to the direction of the tensile force.

In the crystals where the hydrogen bonds are perpendicular to the stretching direction, the hydrogen bonds would experience a compressive force, and this should cause a shift of the NH stretching peak toward lower frequencies. Such a negative frequency shift is not observed in the perpendicularly polarized spectra of Figure 9. Furthermore, Figure 6 indicates that the entire NH peak area broadens and shifts toward higher frequencies with strain: no significant increase in the intensity of the low-frequency end of the NH peak at higher strains (compared to the NH peak at 0 strain) was observed. Hence, compressive forces have minimal effect on the hydrogen bonds perpendicular to the stretching direction. Our results are consistent with Chase and Ikeda, who postulated that very little compression of the hydrogen bond will result because of the anisotropy of the intermolecular forces.²³ This is further borne out by computer simulations which show that the calculated H...H distance between methylene groups on adjacent chains is much shorter in the α crystals (2.140 \AA) than in the γ crystals (2.466 \AA) to permit optimal hydrogen bonding between the amide and carbonyl unit.⁸ This reflects greater repulsion between methylene units on adjacent α chains connected by hydrogen bonds; consequently, compressive forces along the hydrogen

bond direction will have less effect on the hydrogen bonds than tensile forces.

The authors found that peak broadening with frequency shifting took place in the spectra when the polarizer direction is parallel to the stretching direction, similar to Figure 6a. Insignificant amount of broadening occurred in the perpendicular direction. These results show that the broadening results primarily from the α crystals in which the NH bonds are aligned parallel to the stretching direction. These are the bonds that experience tensile stress. The broadening indicates that there is a distribution of stress level among such hydrogen bonds which were formed from these NH groups. The distribution of stress arises from at least two factors: bond orientation and local environment. The angle that the hydrogen bond makes with the stretching direction will determine how much it is deformed under stress and the amount of frequency shift of the NH stretching band. The modulus of the amorphous regions has been found to be 0.80 GPa in the amorphous regions⁶ and calculated to be approximately 34 GPa along the direction of the hydrogen bonds.⁷ The amount of strain in the crystals will depend on whether the crystals and amorphous regions are arranged in series or in parallel along the stretching direction. Furthermore, the crystals could be visualized as "particulates" in a "composite" whereby load is transferred from the amorphous regions (the "matrix") to the crystals. From Cox's shear lag model,³⁴ such a crystal would exhibit a nonuniform stress and would result in nonuniform weakening of hydrogen bonds along the stretching direction.

In the amorphous regions where the chains are less constrained than in the crystals, they can rearrange themselves to a more stable configuration to form stronger hydrogen bonds during deformation, such as the stress transfer mechanism proposed by Chase and Ikeda.²³ This would result in a smaller ND and NH frequency shifts.

For the deuterated films with γ crystals, a positive peak shift is also observed up to a strain of 0.04, though the slope is much less than the films with α crystals. The peak shift then goes back to almost zero at higher strains. The γ films that are not deuterated showed exactly the same behavior. In the ND region, however, there are hardly any frequency shifts for the γ film.

4.2. CH₂ Stretching Modes. Figure 10a shows the frequency shift vs strain curve of the CH₂ asymmetric stretching mode for the nylon-6 films. This peak contains contributions from both the amorphous and crystalline regions. A linear relation is observed for the α films. The peak shifts toward lower wavenumbers with increasing strain. There is negligible frequency shift for the γ films. Figure 10b shows the frequency shift data vs stress. For the α films, the curves are linear up to the stresses corresponding to the strain of 0.04, and then the slopes become steeper at higher stresses.

Parts a and b of Figure 11 show the curves of frequency shift vs strain and stress, respectively, of the CH₂ symmetric stretching mode for the α and γ films. The data are very similar to that of the CH₂ asymmetric stretching vibration—a negative shift is observed for the α films, and there is hardly any shift for the γ films.

The area under the CH₂ stretching peaks contains contributions from both the α crystals and amorphous regions. The broadness of the peaks and its multicomponent nature makes the data analysis difficult. One

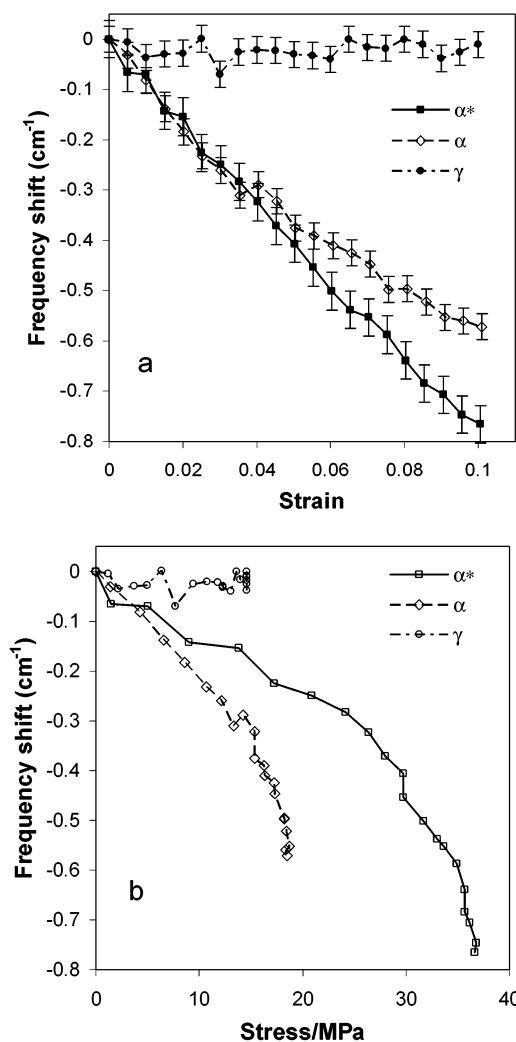


Figure 10. Plot of frequency shift of CH₂ asymmetric stretching vibration in nylon-6 films vs (a) strain and (b) stress. The asterisks indicate deuterated films. The error bars are also shown for each curve.

possible explanation for the frequency shift of the CH₂ stretching mode is a change in the configuration of the amorphous regions during deformation. Chase and Ikeda saw a negative monopolar peak in their dynamic dichroism data and concluded that there is alignment of the polymer backbone in the stretching direction since the transition dipole moments of the CH₂ stretching vibrations are perpendicular to the backbone.²³ Other researchers have also shown that both the frequency and intensity of the CH₂ stretching bands are sensitive to conformation in both hydrocarbon and alkylamino chains.³⁵⁻³⁷

Another possible cause for the observed frequency shift is due to changes in the crystalline phase. The authors have shown earlier that the tensile deformation has greatest effect on the frequency shift of the NH stretching mode in the α crystalline regions than in the amorphous regions. It is known that α crystals have a higher density than γ crystals, and computer simulations have shown that there is substantial repulsion between CH₂ groups in the α crystals due to hydrogen bonding.⁸ Weakening of the hydrogen bond through separation of the two chains hydrogen-bonded to each other would cause changes in the CH bond lengths and hence vibrational frequency due to reduced repulsion.

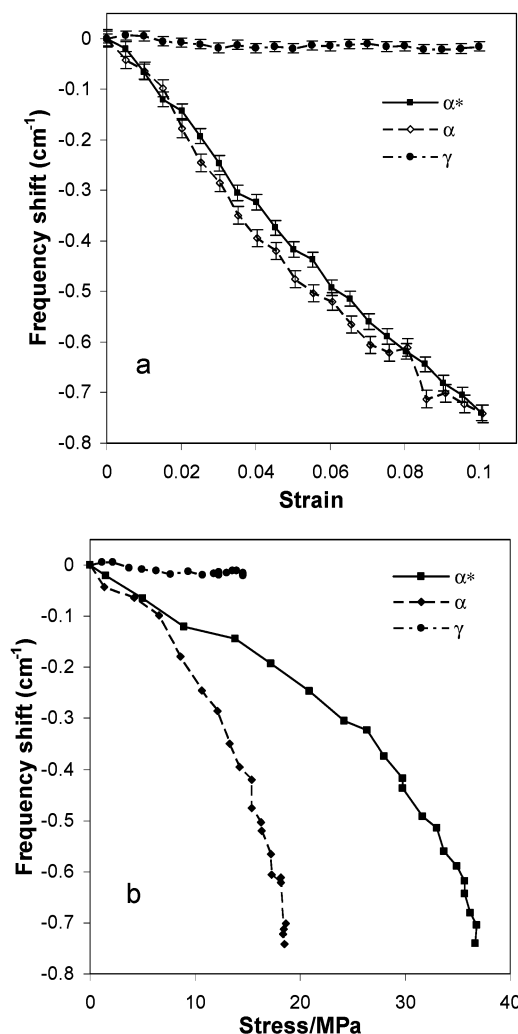


Figure 11. Plot of frequency shift of CH₂ symmetric stretching vibration in nylon-6 films vs (a) strain and (b) stress. The asterisks indicate deuterated films. The error bars are also shown for each curve.

The authors tentatively attribute the observed frequency shifts to the second effect for three reasons. First, the CH₂ stretching peaks of polyethylene underwent a positive frequency shift under hydrostatic pressure.^{38,39} We would therefore expect the opposite to occur when there is an increase in interchain distance between two chains that have substantial repulsion between them. Second, the gauche-to-trans transformation in the amorphous regions does not always cause a decrease in the CH₂ stretch frequency; it can lead to a frequency increase depending on the type of gauche configuration.^{35,37} The authors consistently observed negative shifts of the same magnitude in the CH₂ stretching bands in the deformation experiments. Finally, in the γ films whereby the CH₂ stretch peaks also contain contributions from the crystalline and amorphous regions, the CH₂ stretch frequency shifts are negligible upon application of stress, as shown in Figures 10 and 11. Hence, it can be deduced that the CH₂ stretching vibrations in the amorphous regions undergo negligible frequency shift. Therefore, the downward shifts of the CH₂ stretching mode in the α films are likely to be caused by the crystalline regions. This would indicate that in the α films the CH bond force constant decreases during deformation. As these events are taking place in the crystalline regions, chain align-

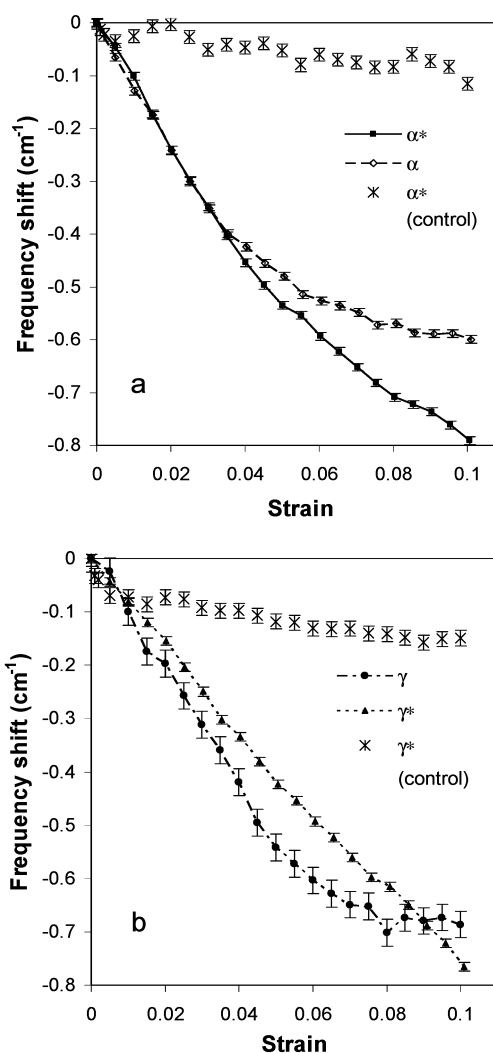


Figure 12. Plot of frequency shift vs strain of the amide II mode in nylon-6 films containing mainly (a) α crystals and (b) γ crystals. The asterisks indicate deuterated films. For the control curves, as the sample was not stretched, each point is plotted at the strain corresponding to the same point in time of the experimental progress. The error bars are also shown for each curve.

ment could still occur in the amorphous regions, leading to changes in peak height.

4.3. Amide II Vibrational Mode. In the α films the frequency of the amide II mode is at 1544 cm⁻¹. Upon deuteration, the area under this peak contains contributions from the crystalline region only, and the peak shifts a little to 1545 cm⁻¹. Figure 12a shows the frequency shift vs strain curve of the amide II vibration for the α films. They show a monotonic decrease in frequency with strain and with stress. The amide II vibration is a complex mode. In polyglycine I the potential energy distribution for the amide II mode is 43% NH in-plane bending, 31% CN stretching, 13% C=O out-of-plane bending, and 12% C_αC stretching.⁴⁰ Its relation with stress and strain is too complicated to analyze. However, two points are worth noting. First, in studies by Skrovanek et al. on an amorphous polyamide, nylon-11 and nylon-12,^{32,41} they found that with increasing temperature the NH stretching peak shifts to higher frequencies and the amide II peak shifts to lower frequencies as the hydrogen bonds are weakened. Second, in small molecules such as *N*-methylacetamide and formamide, the formation of hydrogen bonds is

accompanied by a decrease in NH stretching frequency and an increase in NH in-plane bending frequency, with the amount of upward shift smaller than the downward shift of the stretching modes.⁴² We observe a similar phenomenon here. Therefore, we tentatively attribute the shift of the amide II peak to the lowering of the NH in-plane bending frequency (which is a major component of the amide II mode) as a result of the weakening of the hydrogen bonds due to increased stress.

In the γ films the frequency of the amide II mode is at 1562 cm^{-1} . Upon deuteration, the area under this peak contains contributions from the crystalline region only, and the peak shifts a little to 1565 cm^{-1} . Figure 12b shows the peak shift vs strain curve of the amide II vibration for the γ films. As in the α films, the frequency also showed a negative shift with strain and with stress. The amount of shift of the amide II mode in γ films is higher than that of any other vibrations. This indicates the effects of stress on the film, which is not readily observed in other vibrational modes. Along the same lines of argument as for the α films, the negative shift with stress (or strain) could be attributed to the lowering of the NH in-plane bending frequency as a result of the weakening of hydrogen bonds. In this case, however, the amount of upward shift in the NH stretching vibration is less than the downward shift of the amide II mode at low strains.

The protonation of some of the ND group in the amorphous regions as a result of exchange with atmospheric water vapor also caused a negative frequency shift of the amide II mode with time in both the deuterated α and γ films. This resulted in an error of not more than 17% and 30% for the α and γ films, respectively.

4.4. Correlating Frequency Shifts with Bond Lengths. It is known that the frequency of the NH stretching mode is related to characteristics of the hydrogen bond such as bond length and angle.⁴³ Such an analysis is helpful to gain some understanding of the local strain experience by the crystals. It is recognized that such an approach can only be semiquantitative at best for two important reasons: (a) the frequency at the peak maximum is only representative of a distribution that has different bond lengths and angles locally and different orientation macroscopically; (b) the morphologies of the films are not well-characterized, i.e., the film is not ultradrawn with preferred orientation of the crystals and amorphous regions. This is because the requirement for the absorbance of the peaks be less than or equal to 1 necessitates a processing method that produces thin films with these characteristics. For the NH stretching band, however, the authors have demonstrated that it is the hydrogen bonds aligned preferentially along the stretching direction which are responsible for its frequency shift, a result which will make the analysis more meaningful.

4.4.1. NH Stretching Mode in Deuterated α Films. To correlate the NH frequency shift of the α crystals of the deuterated nylon-6 films in Figure 7 with changes in the N-H...O distance, the analytical model of Schroeder and Lippincott for a linear N-H...O system is used (a summary of the equations involved is reproduced in the Appendix).⁴³ This model is valid for the range of hydrogen bond lengths in crystalline nylon-6 but would break down at longer hydrogen bond distances where the hydrogen bond is weak. The authors chose such a model based upon the FTIR results,

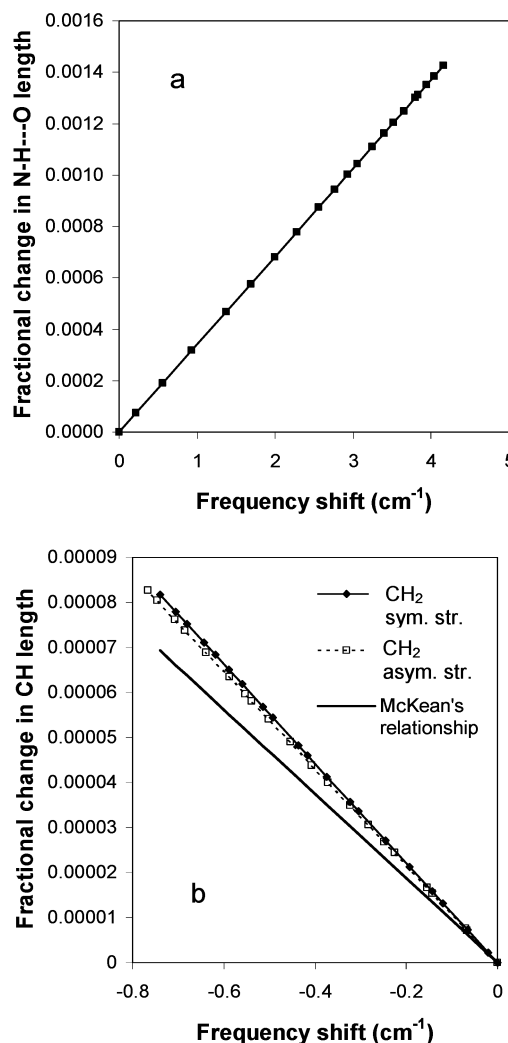


Figure 13. Plot of the fractional change in the (a) N-H...O bond distance and (b) CH bond length of the α crystals in deuterated nylon-6 films vs frequency shift of the respective stretching vibrations. In (b), the CH₂ symmetric and asymmetric stretching vibrations are represented by diamond and square symbols, respectively. The thick line shows the results of calculations based on McKean's relationship.

geometry considerations of the deformation process, and the fact that the N-H...O angle has not been determined experimentally, while simulations utilizing model compounds have produced a wide range of angles from 175° to 106° .^{9,44,45} The N-H...O distance before deformation is calculated to be 2.959 \AA , in good agreement with simulations⁸ and the 2.98 \AA reported by Malta et al.⁴⁶ but shorter than the 2.81 \AA reported by Holmes et al.²⁵ By making use of the NH stretching frequencies at subsequent stresses as input to calculate the N-H...O distance, we obtain Figure 13a, which shows the fractional change of the N-H...O distance vs the NH frequency shift. The graph is linear over the entire range of frequency shifts, showing that the length change is very small, and it is possible to correlate the frequency shifts directly with changes in the hydrogen bond length. The fractional change in N-H...O length is small compared to the macroscopic strain experienced by the film. This could indicate that a significant contribution to the macroscopic strain comes from the amorphous region, consistent with the fact that the measured moduli of the α films ($427\text{--}600\text{ MPa}$) are close to the literature modulus of the amorphous regions

(0.8 GPa).⁶ On the basis of these values, it is reasonable to assume that the amorphous regions and crystalline regions are arranged in series along the stretching direction. We can then estimate from eq 1 a value for α of 100 cm⁻¹/GPa. This value is an order of magnitude higher than that of the C–C stretching band of the axial C–C bond in isotactic polypropylene (–15.8 cm⁻¹/GPa). The high sensitivity of the NH stretching frequency to external stress makes the FTIR technique useful to study micromechanics in hydrogen-bonded systems such as other nylons and poly(vinyl alcohol).

Figure 8 indicates that the frequency shift of the ND stretching mode in the amorphous region is much smaller in extent than that of the NH stretch in the crystals. Therefore, significant rearrangements of the polymer chains can take place in the amorphous region to re-form strong hydrogen bonds, i.e., a final configuration that has the best hydrogen bonding.

In this model the N–H...O bond angle is assumed to be linear, and because of the uncertainty in the model of the hydrogen bond potential, we have plotted fractional change in length rather than the absolute value. Similar results are expected for different hydrogen bond potentials. Our results show that this spectroscopic method is capable of measuring such small distance changes in hydrogen bond length during deformation.

4.4.2. CH₂ Stretching Mode in α Films. The CH₂ asymmetric and symmetric stretching vibration of the deuterated α films is modeled simply as a C–H stretching mode. A Morse potential is utilized for the CH bond:⁴⁷

$$U(\Delta r) = D[1 - \exp(-\eta\Delta r)]^2 \quad (6)$$

where U is the potential energy of the bond, D is the depth of the potential well, and Δr is the change in length of the bond. η is a constant such that the force constant k_0 of the bond in its equilibrium position ($\Delta r = 0$) is given by $k_0 = 2D\eta^2$. The force constant k at a given change in length of the bond is given by

$$k = 2\eta^2 D[2 \exp(-2\eta\Delta r) - \exp(-\eta\Delta r)] \quad (7)$$

The C–H vibrational frequency at the new bond length is then given by

$$\omega/\omega_0 = (k/k_0)^{0.5} \quad (8)$$

where ω_0 is the CH stretching frequency at 0 strain (or $\Delta r = 0$) and ω is the frequency at a given strain (or Δr). The following force field parameters for nylon-6 from simulation results were utilized: the equilibrium bond length $r_0 = 1.076$ Å, $k_0 = 726.71$ kcal/(mol Å²), and $D = 95.1$ kcal/mol.⁸ Using the CH₂ stretching frequencies at different stresses as input, the change in CH bond length can be calculated from eqs 6–8. Figure 13b shows the fractional change in the CH bond length with CH₂ stretch frequency shift. The values obtained are very similar to those obtained from McKean's relationship:

$$r_0 (\text{Å}) = 1.402 - 0.0001035\nu(\text{CH})^{\text{is}} \quad (9)$$

where r_0 is the CH bond length and $\nu(\text{CH})^{\text{is}}$ is the isolated CH stretching frequency.⁴⁸ The curve is linear throughout the entire range of peak shift for both the asymmetric and symmetric stretches. The frequency shifts therefore can be directly correlated with the CH bond length, and the fractional changes in the CH bond

length are very small in this range of peak shifts. The X-ray method of Sakurada et al. was able to measure fractional changes in the lattice distance up to 0.02%.² We are able to measure smaller changes in bond distances (less than 0.001%) with the FTIR method, subject to the limitations of the bond potential.

5. Molecular Picture of Deformation in α and γ Crystals

The α crystals consist of hydrogen-bonded sheets stacked upon one another. The hydrogen bonds hold the chains together within the sheets. During tensile deformation, the chains in each hydrogen-bonded sheet are pulled apart, resulting in an increase in the hydrogen bond (N–H...O) distance, thereby weakening the hydrogen bond. Consequently, the N–H bond strength is decreased, resulting in an upward shift of the NH stretching vibration and downward shift of the amide II mode. Polarized FTIR spectra indicate that the upward shift of the NH stretch peak is due to crystals where the NH bonds are preferentially aligned along the deformation direction. The crystals in which the hydrogen bonds are perpendicular to the stretching direction virtually do not contribute to the frequency shift.

The simultaneous downward shift in the CH₂ stretching frequency is interesting because the CH bonds, unlike the hydrogen bonds, are not expected to bear any loads. The authors have correlated such a negative shift to an increase in bond length. Simulations of α crystals of nylon-6 have indicated that the methylene groups are not optimally packed, resulting in very close H...H distances and greater repulsion between methylene units on adjacent chains.⁸ The tight packing of the methylene segments is thought to allow for the formation of the best hydrogen bonds. When the crystals are deformed, thereby weakening the hydrogen bonds, the methylene groups are not as constrained and the CH bond length can increase toward the optimal configuration. Since the CH bonds do not bear any load, the frequency shifts of the CH₂ stretching modes are therefore a linear function of strain instead of stress.

The fractional change in CH bond length is much smaller than the corresponding fractional change in N–H...O length at a given strain. This can be accounted for by the presence of a potential field between nonbonded H...H pairs, resulting in a repulsive force between methylene groups on adjacent chains.

The lack of significant frequency shifts, particularly for the NH stretching vibration, in the films with γ crystals (except the amide II mode) is surprising. Computer simulations have shown that the spacing of the methylene groups is optimal in the γ phase, unlike the closer packing in the α crystals.⁸ It would therefore be unlikely that deformation would affect the packing in the γ crystals. This is borne out by negligible frequency shift observed for the CH₂ stretching modes in Figures 10 and 11. Since the frequency shift can be correlated to a change in the CH bond length in section 4.4.2, there is then little change in CH distances with deformation. Figure 7 shows that the upward shift in NH stretching frequency with stress is much smaller for the films with the γ crystals compared to that of the α crystals. If the hydrogen bonds in the γ crystals are weakened during deformation, then this result appears to contradict literature data which have shown that hydrogen bonding in the γ crystals has the same effect

of increasing modulus as in the α crystals.⁷ One possible explanation is the mechanical properties of the films are affected by the chemical treatment used to form γ crystals. Another reason is that the hydrogen bonds in the γ crystals are formed between sheets. Since there is preferential alignment of the α crystals with hydrogen bonds parallel to the film surface in the initial film, the chemical treatment to form γ crystals would result in the hydrogen bonds being arranged at an angle to the film surface. Tensile deformation could affect the hydrogen bond in such a manner as to render the NH stretching frequency unchanged. As the NH stretching peak of the γ films is wider than that of the α films (Figure 3c), it is also possible that there may be frequency shifts, but they are masked by the broad peak. Further work is necessary to investigate this effect.

6. Conclusions

There are some important ramifications of this work:

(a) Stress-induced frequency shifts of FTIR vibrations related to hydrogen bonds (NH stretch and amide II) in nylon-6 under tensile deformation have been observed. Contributions from the crystalline and amorphous regions have been distinguished. Furthermore, the effects of stress on crystals oriented at different angles relative to the stretching direction have been observed to be different.

(b) In the α crystals of nylon-6 the NH stretching mode shifts to higher frequencies and broadens when the NH bonds in the crystals are parallel to the stretching direction. The amide II mode shifts toward lower frequencies with stress. This is consistent with the weakening and lengthening of hydrogen bonds which have a favorable orientation relative to the tensile direction. This interchain separation reduces the repulsion between methylene units. The resulting crystal structure at higher stress therefore has longer N-H...O and CH bonds. The fractional change in hydrogen bond length is much larger than that of the CH bond. The FTIR technique enables the changes in X-H bond length as small as 0.001% to be observed.

(c) In the amorphous regions of the deuterated α and γ films there is little frequency shifting of the ND stretching vibration. The chains have more mobility to adopt the most favorable hydrogen bonds configuration during deformation.

(d) The frequency shift of the NH stretching vibration can be very useful to study mechanics of deformation in hydrogen-bonded systems based on the following reasons: (i) the NH stretching vibration at 3300 cm^{-1} is generally uncomplicated by contributions from other vibrations, (ii) it is sensitive to stress due to the large frequency shift coefficient (α) of 100 $\text{cm}^{-1}/\text{GPa}$, (iii) it can be correlated to changes in hydrogen bond distances and hence to the amount of strain in the crystal, and (iv) it is directional and depends on the orientation of the NH bond to the external stress. This method can also be extended to other hydrogen-bonded systems such as poly(vinyl alcohol).

Acknowledgment. This work was sponsored by the DURINT on Microstructure, Processing and Mechanical Performance of Polymer Nanocomposites, Air Force Contract F49620-01-1-0447. The authors thank Dr. J. S. Shelley for providing the nylon-6 materials and Professor R. E. Cohen for discussion and the use of the spin-casting equipment.

Appendix

Potential Function Model of Linear N-H...O Hydrogen Bonds.⁴³ The N-H and H...O bond lengths are represented by r and r^* , respectively. They are related by the following equation:

$$\Delta r = r - r_0 = \frac{D_0^* n^*}{D_0 n} e^{\alpha - \beta} \frac{r^2 (r^* - r_0^*) (r^* + r_0^*)}{r^{*2} (r + r_0)}$$

The NH stretching frequency ω_H is given by

$$\frac{\omega_H}{\omega_0} = \sqrt{\frac{k_H}{k_0}} = \sqrt{r_0 e^{-\alpha} \frac{r_0^2 - \frac{\alpha}{2} (r + r_0)^2}{r^3} + r_0 \frac{D_0^* n^*}{D_0 n} e^{-\beta} \frac{r_0^{*2} - \frac{\beta}{2} (r^* + r_0^*)^2}{r^{*3}}}$$

where

$$\alpha = n(r - r_0)^2 / 2r$$

$$\beta = n^*(r^* - r_0^*)^2 / 2r^*$$

$$n = k_0 r_0 / D_0$$

$$n^* = g n$$

$$D_0^* = k_0^* r_0^* / n^*$$

D_0 and D_0^* are the NH and OH bond dissociation energy, respectively, r_0 and r_0^* are the NH and OH bond lengths, respectively, in the absence of hydrogen bonding, ω_0 is the NH stretching frequency in the absence of hydrogen bonding, k_0 and k_0^* are the NH stretching force constants, respectively, in the absence of hydrogen bonding, and g is an empirically determined parameter. The values of these constants have been given in Table 1 of ref 43 as follows: $D_0 = 104 \text{ kcal/mol}$, $n = 9.30 \times 10^8 \text{ cm}^{-1}$, $n^* = 13.15 \times 10^8 \text{ cm}^{-1}$, $r_0 = 0.99 \text{ \AA}$, $r_0^* = 0.96 \text{ \AA}$, $k_0 = 6.42 \times 10^5 \text{ dyn/cm}$, $k_0^* = 7.76 \times 10^5 \text{ dyn/cm}$, and $\omega_0 = 3500 \text{ cm}^{-1}$.

References and Notes

- Lin, L.; Argon, A. S. *Macromolecules* **1992**, *25*, 4011–4024.
- Sakurada, I.; Kaji, K. *J. Polym. Sci., Part C* **1970**, *31*, 57–76.
- Lewis, E. L. V.; Ward, I. M. *J. Macromol. Sci., Phys.* **1980**, *B18*, 1–46.
- Leung, W. P.; Ho, K. H.; Choy, C. L. *J. Polym. Sci., Polym. Phys. Ed.* **1984**, *22*, 1173–1191.
- Lewis, E. L. V.; Ward, I. M. *J. Macromol. Sci., Phys.* **1981**, *B19*, 75–107.
- Prevorsek, D. C.; Harget, P. J.; Sharma, R. K.; Reimschuessel, A. C. *J. Macromol. Sci., Phys.* **1973**, *B8*, 127–156.
- Tashiro, K.; Tadokoro, H. *Macromolecules* **1981**, *14*, 781–785.
- Dasgupta, S.; Hammond, W. B.; Goddard III, W. A. *J. Am. Chem. Soc.* **1996**, *118*, 12291–12301.
- Peeters, A.; Van Alsenoy, C.; Bartha, F.; Bogar, F.; Zhang, M.-L.; Van Doren, V. E. *Int. J. Quantum Chem.* **2002**, *87*, 303–310.
- Galeski, A.; Argon, A. S.; Cohen, R. E. *Macromolecules* **1991**, *24*, 3945–3952.
- Galeski, A.; Argon, A. S.; Cohen, R. E. *Macromolecules* **1991**, *24*, 3953–3961.
- Galeski, A.; Argon, A. S.; Cohen, R. E. *Macromolecules* **1988**, *21*, 2761–2770.
- Murthy, N. S.; Grubb, D. T. *J. Polym. Sci., Part B: Polym. Phys.* **2002**, *40*, 691–705.

- (14) Murthy, N. S.; Bray, R. G.; Correale, S. T.; Moore, R. A. F. *Polymer* **1995**, *36*, 3863–3873.
- (15) Penel-Pierron, L.; Seguela, R.; Lefebvre, J.-M.; Miri, V.; Depecker, C.; Jutigny, M.; Pabiot, J. *J. Polym. Sci., Part B: Polym. Phys.* **2001**, *39*, 1224–1236.
- (16) Zhurkov, S. N.; Vettegren, V. I.; Novak, I. I.; Kashincheva, K. N. *Dokl. Akad. Nauk USSR* **1967**, *176*, 623–626.
- (17) Zhurkov, S. N.; Vettegren, V. I.; Korsukov, V. E.; Novak, I. I. *Fiz. Tverd. Tela* **1969**, *11*, 290–295.
- (18) Vettegren, V. I.; Novak, I. I.; Friedland, K. J. *Int. J. Fract.* **1975**, *11*, 789–801.
- (19) Wool, R. P.; Statton, W. O. *J. Polym. Sci., Polym. Phys. Ed.* **1974**, *12*, 1575–1586.
- (20) Wool, R. P.; Boyd, R. H. *J. Appl. Phys.* **1980**, *51*, 5116–5124.
- (21) Tashiro, K.; Minami, S.; Wu, G.; Kobayashi, M. *J. Polym. Sci., Part B: Polym. Phys.* **1992**, *30*, 1143–1155.
- (22) Kischel, M.; Kisters, D.; Strohe, G.; Veeman, W. S. *Eur. Polym. J.* **1998**, *34*, 1571–1577.
- (23) Chase, D. B.; Ikeda, R. M. *Macromol. Symp.* **1999**, *141*, 217–226.
- (24) Reynolds, F. S. C. J.; Sternstein, S. S. *J. Chem. Phys.* **1964**, *41*, 47–50.
- (25) Holmes, D. R.; Bunn, C. W.; Smith, D. J. *J. Polym. Sci.* **1955**, *17*, 159–177.
- (26) Arimoto, H. J. *Polym. Sci., Part A* **1964**, *2*, 2283–2295.
- (27) Rotter, G.; Ishida, H. *J. Polym. Sci., Part B: Polym. Phys.* **1992**, *30*, 489–495.
- (28) Murthy, N. S.; Stamm, M.; Sibilia, J. P.; Krimm, S. *Macromolecules* **1989**, *22*, 1261–1267.
- (29) Schmidt, P. G. *J. Polym. Sci., Part A* **1963**, *1*, 1271–1292.
- (30) Brandrup, J.; Immergut, E. H., Eds. In *Polymer Handbook*, 3rd ed.; John Wiley and Sons: New York, 1989.
- (31) Sibilia, J. P. *J. Polym. Sci., Part A* **1971**, *9*, 27–42.
- (32) Skrovanek, D. J.; Howe, S. E.; Painter, P. C.; Coleman, M. M. *Macromolecules* **1986**, *19*, 699–705.
- (33) Bretzlaff, R. S.; Wool, R. P. *Macromolecules* **1983**, *16*, 1907–1917.
- (34) Cox, H. L. *Br. J. Appl. Phys.* **1952**, *3*, 72–79.
- (35) Aljibury, A. L.; Snyder, R. G.; Strauss, H. L.; Raghavachari, K. *J. Chem. Phys.* **1986**, *84*, 6872–6878.
- (36) Snyder, R. G. *Macromolecules* **1990**, *23*, 2081–2087.
- (37) Ohno, K.; Nomura, S.-i.; Yoshida, H.; Matsuura, H. *Spectrochim. Acta, Part A* **1999**, *55*, 2231–2246.
- (38) Wu, C.-K.; Nicol, M. *Chem. Phys. Lett.* **1973**, *18*, 83–86.
- (39) Zhao, Y. N.; Wang, J.; Cui, Q. L.; Liu, Z. X.; Yang, M. L.; Shen, J. C. *Polymer* **1990**, *31*, 1425–1428.
- (40) Moore, W. H.; Krimm, S. *Biopolymers* **1976**, *15*, 2439–2464.
- (41) Coleman, M. M.; Skrovanek, D. J.; Painter, P. C. *Makromol. Chem., Macromol. Symp.* **1986**, *5*, 21–33.
- (42) Pimentel, G. C.; McClellan, A. L. In *The Hydrogen Bond*; W. H. Freeman and Co.: San Francisco, 1960; pp 118–125.
- (43) Schroeder, R.; Lippincott, E. R. *J. Phys. Chem.* **1957**, *61*, 921–928.
- (44) Li, Y.; Goddard III, W. A. *Macromolecules* **2002**, *35*, 8440–8455.
- (45) Bernado, P.; Aleman, C.; Puiggali, J. *Eur. Polym. J.* **1999**, *35*, 835–847.
- (46) Malta, V.; Cojazzi, G.; Fichera, A.; Ajo, D.; Zannetti, R. *Eur. Polym. J.* **1979**, *15*, 765–770.
- (47) Tashiro, K.; Gang, W.; Kobayashi, M. *J. Polym. Sci., Part B: Polym. Phys.* **1990**, *28*, 2527–2553.
- (48) McKean, D. C. *Chem. Soc. Rev.* **1978**, *7*, 399–422.

MA034213V